

## Monoclinic nearly stoichiometric wüstite at low temperatures

HELMER FJELLVÅG,<sup>1</sup> BJØRN C. HAUBACK,<sup>2</sup> TOM VOGT,<sup>3</sup> AND SVEIN STØLEN<sup>1,\*</sup>

<sup>1</sup>Department of Chemistry, University of Oslo, Postbox 1033, N0315 Oslo, Norway

<sup>2</sup>Institute for Energy Technology, Kjeller, Norway

<sup>3</sup>Physics Department, 2-21, Building 510B, Brookhaven National Laboratory, Upton, New York 11973-5000, U.S.A.

### ABSTRACT

The crystallographic and magnetic structures of Fe<sub>0.99</sub>O at 10 K have been determined by high-resolution neutron powder diffraction. Fe<sub>0.99</sub>O is found to be monoclinic, space group *C2/m*, with unit-cell dimensions  $a = 5.2615(1)$ ,  $b = 3.0334(1)$ ,  $c = 3.0602(1)$  Å, and  $\beta = 124.649(2)^\circ$ . The Fe-O distances in the distorted FeO<sub>6</sub> octahedron are  $2.154 \text{ \AA} \times 4$  and  $2.165 \text{ \AA} \times 2$ . The magnetic unit cell is obtained by doubling one of the crystallographic axes,  $a$  (magn) =  $a_m$ ,  $b$  (magn) =  $b_m$ , and  $c$  (magn) =  $2c_m$ . The refined magnetic components at 8 K are  $M_x = 2.7(1) \mu\text{B}$ ,  $M_y = -0.9(2) \mu\text{B}$ , and  $M_z = 4.77(2) \mu\text{B}$ , with resultant  $M = 4.03(2) \mu\text{B}$ .

### INTRODUCTION

Wüstite is antiferromagnetically ordered at temperatures below about 195 K. The magnetic order-disorder transition changes character with composition of Fe<sub>1-x</sub>O and becomes strongly cooperative for nearly stoichiometric FeO (Stølen et al. 1996). The magnetic structure of Fe<sub>1-x</sub>O has been studied by neutron diffraction methods. The spins of the Fe<sup>2+</sup> ions are antiferromagnetically ordered within (111) and the main magnetic component is along [111]. However, in addition to this parallel component ( $3.8 \mu\text{B}$  for Fe<sub>0.99</sub>O), a smaller perpendicular component is observed ( $1.3 \mu\text{B}$  for Fe<sub>0.99</sub>O) (Fjellvåg et al. 1996). The ordered moment is significantly lower in iron-reduced samples (Shull et al. 1951; Roth 1960; Battle and Cheetham 1979). In these, the introduction of Fe<sup>3+</sup> atoms at tetrahedral sites gives rise to small magnetic clusters where the closest Fe neighbors are arranged antiferromagnetically relative to the Fe<sup>3+</sup> atoms. However, these clusters are disordered and do not contribute to the ordered moment (Battle and Cheetham 1979). The antiferromagnetic ordering is accompanied by a symmetry reduction. The paramagnetic phase has an NaCl-type structure (space group *Fm $\bar{3}$ m*), whereas the low temperature phase is reported to be rhombohedrally distorted (space group *R $\bar{3}$* ). The degree of distortion (deviation of  $\alpha$  from  $60^\circ$ ) appears to increase with increasing Fe content (Toombs and Rooksby 1950; Willis and Rooksby 1953).

The present high-resolution powder neutron diffraction study of Fe<sub>0.99</sub>O at low temperatures is intended to contribute to a correct crystallographic understanding of magnetically ordered wüstite and was initiated on the basis of problems with Rietveld refinement of high-pressure X-ray diffraction data for

the intermediate-pressure phase of FeO. It has long been assumed that the magnetically ordered low-temperature phase is stabilized by pressure and that this is the phase that becomes stable at ambient temperature at around 16 GPa. The magnetic symmetry that results from published descriptions indicates a lower than rhombohedral symmetry. It is interesting to note that monoclinic descriptions have been advanced for CoO where the magnetic structure also has significant parallel and perpendicular components (Daniel and Cracknell 1969).

### EXPERIMENTAL METHODS

Two samples were synthesized and studied. The preparation of sample 1 was described previously (Grønvold et al. 1993; Stølen et al. 1995, 1996). The sample was prepared by careful disproportionation of a non-stoichiometric wüstite with composition Fe<sub>0.937</sub>O in a step-wise heated adiabatic calorimeter. This instrument allows us to monitor the extent of reaction through detection of the reaction heat flow. Sample 2 was prepared similarly by annealing the sample at 500 K for 6 h (Stølen et al. 1995). While the first method allows us to prepare a sample rich in Fe<sub>0.99</sub>O, the second approach gave us a less ideal sample with a much smaller fraction of Fe<sub>0.99</sub>O.

Powder neutron diffraction data for sample 1 were collected at 10 and 298 K at the High Flux Beam Reactor at Brookhaven National Laboratory, New York, with the high-resolution neutron powder diffractometer H1A. Monochromatic neutrons with wavelength  $1.8857 \text{ \AA}$  were obtained from a focusing Ge(511) monochromator. Sixty-four <sup>3</sup>He detectors allowed data collection from  $2\theta = 10$  to  $155^\circ$  in steps of  $\Delta 2\theta = 0.05^\circ$ . Similarly, data for sample 2 were collected at 8 K with the high-resolution PUS diffractometer at the JEEP II reactor, Kjeller, Norway. A Displex cooling machine was used and the sample was placed in a 5 mm cylindrical V can. Neutrons of wavelength

\* E-mail: svein.stolen@kjemi.uio.no

1.5554 Å were obtained from a Ge(511) monochromator. Intensities were collected with two banks of detectors, each consisting of seven position sensitive detectors and covering 20° in 2θ. Data were collected between 5 and 130° in steps of 0.05° 2θ.

The program Fullprof, version 0.5, (Rodríguez-Carvajal 1993) was used for the Rietveld-type profile refinements. Background points were selected manually and the peak shapes were described by mixed Gaussian-Lorentzian functions.

## RESULTS AND DISCUSSION

The results clearly demonstrate that the earlier crystallographic description of the low temperature structure of Fe-rich wüstite is not fully correct. However, this could not have been detected in the earlier experiments, because the crucial diffraction features distinguishing different models require data with high resolution at high scattering angles. In order not to be mistaken due to possible reflections stemming from cryostat or unknown impurities, repeated experiments were conducted for two different samples on two different instruments with two different wavelengths.

As in our earlier studies of nearly stoichiometric wüstite (Stølen et al. 1996; Fjellvåg et al. 1996), the presently studied samples are three phase mixtures of Fe, nearly stoichiometric FeO and Fe<sub>3</sub>O<sub>4</sub>. Figure 1 shows a selected part of the observed and calculated (using the reported rhombohedral description of wüstite) diffraction pattern with focus on scattering from Fe<sub>0.99</sub>O. By comparing the two data sets, the splitting and extra peaks could not be explained by cryostat or unknown impurities. The rhombohedral description cannot explain the peak splitting at around 2θ = 122°. The observed pattern could, however, be fit using a monoclinic structure description (see observed and calculated diffraction patterns in Fig. 2). The intensity ratio of the split peaks is the same in both samples and due to the wüstite component of the three-phase mixture. The monoclinic unit cell relates to the cubic cell as follows:  $a_m = -1/2a_c - 1/2b_c + c_c$ ,  $b_m = 1/2a_c - 1/2b_c$ , and  $c_m = 1/2a_c + 1/2b_c$ . The unit cell has half the volume of the NaCl-type unit cell,

**TABLE 1.** Unit-cell dimensions (crystallographic cell), atomic coordinates, mass fractions, and reliability factors as obtained from Rietveld refinement of powder neutron diffraction data for both three-phase samples

Parameter	Sample 1 (BNL, 10 K)	Sample 2 (Kjeller, 8 K)
$a$ (Fe <sub>0.99</sub> O)	5.2615(2)	5.2642(7)
$b$ (Fe <sub>0.99</sub> O)	3.0334(1)	3.0327(4)
$c$ (Fe <sub>0.99</sub> O)	3.0602(1)	3.0626(4)
$\beta$ (Fe <sub>0.99</sub> O)	124.649(2)	124.646(9)
$a$ (Fe)	2.855(1)	2.8604(1)
$a$ (Fe <sub>3</sub> O <sub>4</sub> )	8.3851(3)	8.3858(2)
Fraction Fe	0.0022(3)	0.114(1)
Fraction Fe <sub>0.99</sub> O	0.759(2)	0.200(1)
Fraction Fe <sub>3</sub> O <sub>4</sub>	0.239(1)	0.686(3)
$x$ (O) Fe <sub>3</sub> O <sub>4</sub>	0.2534(4)	0.2548(2)
$R_p$	0.056	0.056
$R_{wp}$	0.074	0.076
$R_M$	0.051	0.25
$\chi^2$	4.86	5.8

Notes: Calculated standard deviations are shown in parentheses. Space groups are  $C2/m$  for Fe<sub>0.99</sub>O,  $Fd\bar{3}m$  for Fe<sub>3</sub>O<sub>4</sub>, and  $Im\bar{3}m$  for Fe(bcc).

hence  $Z = 2$ . The refined unit-cell dimensions and atomic coordinates for Fe<sub>0.99</sub>O in space group  $C2/m$  are given in Table 1. There are only minor differences in the crystal structure of Fe<sub>0.99</sub>O as obtained in the rhombohedral vs. monoclinic descriptions. In the rhombohedral model, there are six equivalent Fe-O distances of 2.157 Å in the distorted FeO<sub>6</sub> octahedron, and in the monoclinic model, these become 2.154 Å × 4 and 2.165 Å × 2.

A doubling of one of the crystallographic axes was required in order to explain all magnetic reflections of Fe<sub>0.99</sub>O:  $a$  (magn) =  $a_m$ ,  $b$  (magn) =  $b_m$ , and  $c$  (magn) =  $2c_m$ . This is similar to what is observed for CoO (Daniell and Cracknell 1969). Refinement of the magnetic structure was conducted for the enlarged unit cell, with all atomic coordinates fixed to their ideal positions (as dictated by the  $C2/m$  description). The refined magnetic components at 8 K for Fe<sub>0.99</sub>O are  $M_x = 2.7(1)$  μB,  $M_y = -0.9(2)$

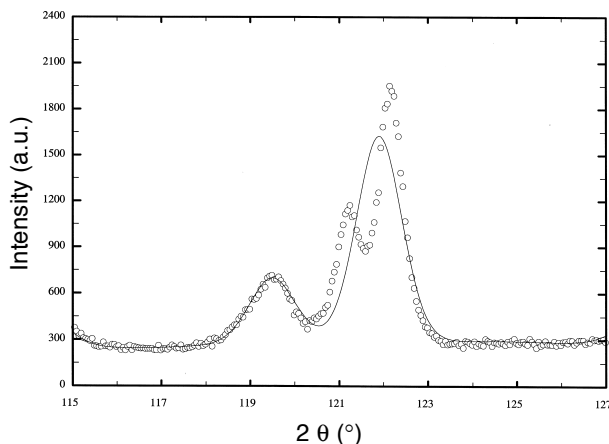


**FIGURE 1.** Observed and calculated powder neutron diffraction intensities for rhombohedral Fe<sub>0.99</sub>O ( $R\bar{3}$ ) ( $\lambda = 1.8857$  Å).

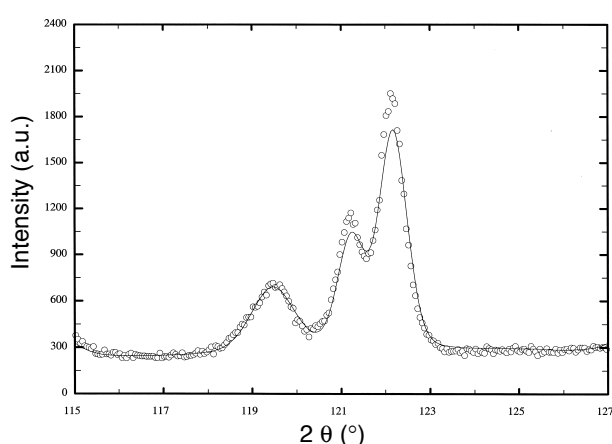


**FIGURE 2.** Observed and calculated powder neutron diffraction intensities for monoclinic Fe<sub>0.99</sub>O ( $C2/m$ ) ( $\lambda = 1.8857$  Å).

$\mu\text{B}$ , and  $M_z = 4.77(2) \mu\text{B}$  with resultant  $M = 4.03(2) \mu\text{B}$ . The magnetic structure is essentially as described previously for the rhombohedral model (Fjellvåg et al. 1996). The refined antiferromagnetic and ferromagnetic components of  $\text{Fe}_3\text{O}_4$  are  $4.2(1)$  and  $3.2(3) \mu\text{B}$ , which comply reasonably well with literature data (Kakol and Honig 1989). The magnetic structure is shown in Figure 3. The overall fit between observed and calculated powder neutron diffraction intensities (BNL data) is shown in Figure 4. The higher magnetic  $R$  factor for the Kjeller data (see Table 1) is due to the smaller fraction of  $\text{Fe}_{0.99}\text{O}$  in addition to somewhat lower instrumental resolution.

The fact that the crystal structure is definitely monoclinic in the antiferromagnetic state is important. The degree of monoclinic distortion may be composition dependent and may be larger for more Fe-rich samples. This is indicated by the earlier diffraction studies, both with respect to the magnetic moment orientation within a rhombohedral model and with respect to deviations from cubic symmetry below  $T_N$ .

Zou et al. (1980) reported a pressure-induced phase transition at 9 GPa and 298 K and suggested that the high-pressure phase was rhombohedral. Later, Yagi et al. (1985) observed the transition at 16 GPa and also suggested a rhombohedral phase at high pressure (to 120 GPa). However, the diffraction

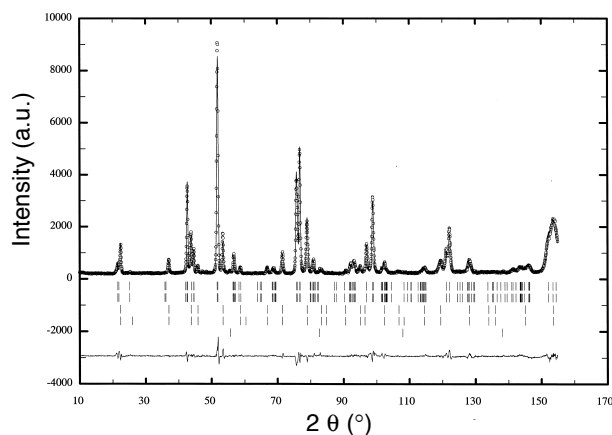


FIGURE 3. Magnetic structure of monoclinic  $\text{Fe}_{0.99}\text{O}$  at 10 K in the magnetic unit cell  $a$  (magn) =  $a_m$ ,  $b$  (magn) =  $b_m$ , and  $c$  (magn) =  $2c_m$ .

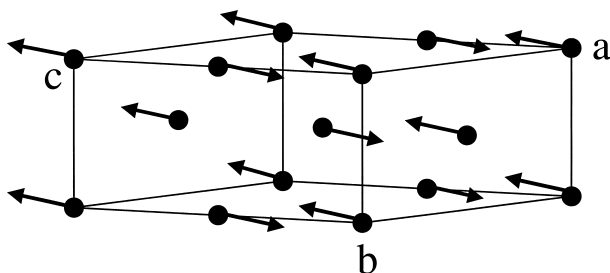


FIGURE 4. Observed, calculated, and difference powder neutron diffraction profiles for monoclinic  $\text{Fe}_{0.99}\text{O}$  ( $C2/m$ ) at 10 K. Marked reflections refer to Fe (bottom),  $\text{Fe}_{0.99}\text{O}$  (magnetic and nuclear), and  $\text{Fe}_3\text{O}_4$  (magnetic and nuclear) ( $\lambda = 1.8857 \text{ \AA}$ ).

pattern calculated for the rhombohedral structure compared poorly with the observed  $d$  spacings (see discussion in Haavik et al. 2000). A recent single-crystal X-ray diffraction study (Mao et al. 1996; Shu et al. 1998), however, claims to prove unequivocally that this high-pressure phase is rhombohedral. In order to explain all observed reflections it was postulated that the cubic low-pressure phase at 18 GPa transforms to four twin domains of the rhombohedral phase. The present monoclinic description of low-temperature  $\text{Fe}_{0.99}\text{O}$  may provide a basis for an alternative description of the high-pressure structure. This leads to the following question: does  $\text{Fe}_{0.99}\text{O}$  (and non-stoichiometric  $\text{Fe}_{1-x}\text{O}$ ) undergo a similar monoclinic distortion when subjected to high pressures?

## ACKNOWLEDGMENT

The work at Brookhaven National Laboratory was supported by the Division of Materials Science, U.S. Department of Energy, under contract no. DE-AC02-98-CH10886.

## REFERENCES CITED

- Battle, P.D. and Cheetham, A.K. (1979) The magnetic structure of non-stoichiometric ferrous oxide. *Journal of Physics C: Solid State Physics*, 12, 337–345.
- Daniel, M.R. and Cracknell, A.P. (1969) Magnetic symmetry and antiferromagnetic resonance in  $\text{CoO}$ . *Physical Review*, 177, 932–941.
- Fjellvåg, H., Grønvold, F., Stølen, S., and Hauback, B.C. (1996) On the crystallographic and magnetic structures of nearly stoichiometric iron monoxide. *Journal of Solid State Chemistry*, 124, 52–57.
- Grønvold, F., Stølen, S., Tolmach, P., and Westrum, E.F., Jr., (1993) Heat capacities of the wüstites  $\text{Fe}_{0.9779}\text{O}$  and  $\text{Fe}_{0.9255}\text{O}$  at temperatures  $T$  from 5 to 350 K. Thermodynamics of the reaction:  $x\text{Fe}(s) + (1/4)\text{Fe}_3\text{O}_4(s) = \text{Fe}_{0.7500+x}\text{O}(s) = \text{Fe}_{1-x}\text{O}(s)$  at  $T = 850 \text{ K}$  and properties of  $\text{Fe}_{1-x}\text{O}$  to  $T = 1000 \text{ K}$ . Thermodynamics of formation of wüstite. *The Journal of Chemical Thermodynamics*, 25, 1089–1117.
- Haavik, C., Stølen, S., Hanfland, M., and Catlow, C.R.A. (2000) Effect of defect clustering on the high-pressure behaviour of wüstite. *High-pressure X-ray diffraction and lattice energy simulations*. *Physical Chemistry Chemical Physics*, 2, 5333–5340.
- Kakol, Z. and Honig, J.M. (1989) Influence of deviations from ideal stoichiometry on the anisotropy parameters of magnetite  $\text{Fe}_{3(1-\delta)}\text{O}_4$ . *Physical Review B*, 40, 9090–9097.
- Mao, H.K., Shu, J., Fei, Y., Hu, J., and Hemley, R.J. (1996) The wüstite enigma. *Physics of the Earth and Planetary Interiors*, 96, 135–145.
- Rodríguez-Carvajal, J. (1993) Recent advances in magnetic structure determination by neutron powder diffraction. *Physica B*, 192, 55–69.
- Roth, W.L. (1960) Defects in the crystal and magnetic structures of ferrous oxide. *Acta Crystallographica*, 13, 140–149.
- Shu, J., Mao, H.-K., Hu, J., Fei, Y., and Hemley, R.J. (1998) Single-crystal X-ray diffraction of wüstite to 30 GPa hydrostatic pressure. *Neues Jahrbuch Mineralogie Abhandlungen*, 172, 309–323.
- Shull, C.G., Strauser, W.A., and Wollan, E.O. (1951) Neutron diffraction by paramagnetic and antiferromagnetic substances. *Physical Review*, 83, 333–345.
- Stølen, S., Glöckner, R., and Grønvold, F. (1995) Nearly stoichiometric iron monoxide formed as a metastable intermediate in a two-stage disproportionation of quenched wüstite. Thermodynamic and kinetic aspects. *Thermochimica Acta*, 256, 91–106.
- Stølen, S., Glöckner, R., Grønvold, F., Atake, T., and Izumisawa, S. (1996) Heat capacity and thermodynamic properties of nearly stoichiometric wüstite from 13 to 450 K. *American Mineralogist*, 81, 973–981.
- Toombs, N.C. and Rooksby, H.P. (1950) Structure of monoxides of some transition elements at low temperatures. *Nature*, 165, 442–443.
- Willis, B.T.M. and Rooksby, H.P. (1953) Change of structure of ferrous oxide at low temperature. *Acta Crystallographica* 6, 827–831.
- Yagi, T., Suzuki, T., and Akimoto, S.-I. (1985) Static compression of wüstite ( $\text{Fe}_{0.98}\text{O}$ ) to 120 GPa. *Journal of Geophysical Research*, 90, B10, 8784–8788.
- Zou, G., Mao, H.-K., Bell, P.M., and Virgo, D. (1980) High pressure experiments on the iron oxide wüstite ( $\text{Fe}_{1-x}\text{O}$ ). *Year Book Carnegie Institution Washington*, 79, 374–376.